International Journal of Impact Engineering 85 (2015) 20–26

Contents lists available at ScienceDirect

International Journal of Impact Engineering

journal homepage: www.elsevier.com/locate/ijimpeng

Analytical formulation of a criterion for adiabatic shear failure

M. Dolinski*, M. Merzer, D. Rittel

Faculty of Mechanical Engineering, Technion, 32000 Haifa, Israel

ARTICLE INFO

Article history:
Received 30 March 2015
Received in revised form
10 June 2015
Accepted 11 June 2015
Available online 20 June 2015

Keywords:
Adiabatic shear bands
Finite elements
Energy criterion
Metallic materials

ABSTRACT

Numerical modeling and prediction of adiabatic shear localization require a criterion that is both robust and simple enough so that it can be implemented into numerical codes. This criterion should have a minimum number of adjustable parameters, each of which being measurable, with sufficient generality to avoid adjustments for each new investigated case.

This paper presents a detailed analytical study of such a criterion formulated in terms of plastic strain energy density. The criterion contains 3 physical parameters: an exponent b and two energy parameters corresponding to the initiation of the shear band and its final failure. It describes both the initiation and the propagation of the damage (shear band) in the dynamically loaded solid, while b represents the damage tolerance characteristics of the material. We show that the general stress–strain relationship decays exponentially (or close to) with ongoing damage, which allows attainment of very large strains in the shear band. A detailed procedure is reported for the experimental identification of each of the above-mentioned parameters, for any value of the exponent b.

The criterion was previously used for dynamic shear localization simulations on empirical grounds [1], that are now firmly established for the first time through a rigorous analysis, including systematic parameters' identification.

1. Introduction

Adiabatic shear banding (ASB) had been studied in numerous works from mathematical, mechanical and metallurgical considerations, for over seven decades. This failure mode plays a major role in dynamic applications such as machining, high-rate metal forming, and particularly in ballistic impacts [2]. Instead of a homogeneous plastic deformation state, the strain gets localized into a narrow plane (band in two dimensions), which leads rapidly and abruptly to catastrophic structural failure. The bands are characterized by both very large shear strains (of the order of 10), and consequently very high local temperatures (several hundred degrees), as a result of thermomechanical coupling effects [3].

The classical explanation for the occurrence of this failure mode was proposed by Zener and Hollomon [4], who pointed out that localization occurs when the thermal softening effect overcomes strain hardening of the material. At this point, a material instability develops and the material loses abruptly its load bearing capability. Based on this premise, attainment of a critical strain is usually considered as a failure criterion [5]. However, earlier work by Dormeval and Ansart [6] examined this concept through a series of experiments involving static pre-loading, followed by dynamic loading. Those authors showed that a critical strain criterion is inadequate to predict the onset of adiabatic shear failure.

Based on similar two-stage experiments, Rittel et al. [7] reached a similar conclusion, but suggested to consider only the dynamic phase of the experiments. Those authors reported that irrespective of the level of quasi-static prestrain, the measured dynamic strain energy density remained quite constant. Those authors consequently proposed a new criterion for dynamic failure, with special emphasis on adiabatic shear bands (ASB). The criterion is based on the dynamic stored energy of cold work instead of the commonly accepted critical strain criterion. This criterion is based on part of the total strain energy density invested in the impacted material. Here, one should mention the work of Mazeau et al. [8] who ranked the susceptibility of various titanium alloys to adiabatic shear failure on the basis of the strain energy density absorbed by the material prior to failure.

Justifications for this criterion are based on the following:

a. The authors showed that the dynamic strain energy (density) to failure is constant for different values of pre-strain, thus a critical strain criterion is not suitable [7].

* Corresponding author.
E-mail address: dolmich@technion.ac.il (M. Dolinski).

http://dx.doi.org/10.1016/j.ijimpeng.2015.06.009
0734-743X/

b. In another work of Rittel and Wang [9], it was shown that the temperature rise prior to instability is of the order of a few tens of degrees. Such an increase is most likely insufficient to cause significant material softening, contrary to the claim of Zener and Hollomon [4].
c. An evaluation of the respective contribution of microstructural changes and thermal softening can be found in Osovski et al. [10]. This study investigates the joint operation of the two softening mechanisms, pointing out that for those materials that exhibit high strength levels and overall low ductility, microstructural softening is likely to kick in prior to any thermal softening, whereas for lower strength materials with a high ductility, provided microstructural evolutions have not occurred, thermal softening is likely to be the dominant factor leading to the instability. Those results are summarized graphically in Fig. 13 of this work [10].
d. Osovski et al. [11] showed that for a range of strain rates, the strain energy density at failure is constant. This stands at odds with the strain criterion which should be adapted for each strain rate in particular, as for example in Zhou et al. [12] and Medyanik et al. [13].

Finally, one should mention recent work, based on molecular dynamics, that added to the feasibility of an energy approach to dynamic shear localization [14].

The numerical implementation of the strain energy density as a failure criterion was carried out recently by Dolinski et al. [1], and by Noam et al. [15]. In the first work, four different laboratory experiments were modeled successfully, both qualitatively and quantitatively. The second work included simulations of scaling of plate response under explosive loading and ballistic perforation, problems which both involve ASB-related failure. However, the strain energy concept was used on a purely empirical basis in those works. Likewise, this approach was also implemented recently for non-metallic materials by Aranda-Ruiz and Loya [16], who successfully reproduced the failure mode transition experiments of polycarbonate performed by Ravi-Chandar et al. [17].

The idea of energy as a failure criterion is not entirely new and has been applied to several cases, including fracture mechanics [18]. The notion of a limited strain energy (density) has been mentioned earlier in works of Farren and Taylor [19] and Taylor and Quinney [20]. However, to our knowledge, no failure criterion based on this exact notion was further developed. There are nevertheless two models for failure in the literature. However they should not be confused with our plastic strain energy density model for the initiation and propagation of adiabatic shear bands.

The first model – a very common failure criterion (C–L) was introduced by Cockcroft and Latham [21]. The C–L criterion: $\int_0^{\varepsilon_{eq}} \sigma_1 d\varepsilon_{eq} \le W_{cr}$ with σ_1 being the maximal principal stress, to be compared with the previous plastic strain energy density criterion [1]: $\int_0^{\varepsilon_{eq}} \sigma_M d\varepsilon_{eq}^P$ with σ_M standing for equivalent Mises stress.

Cockcroft and Latham [21] defined their criterion for *fracture*, based on the maximum principal stress component. When this criterion is met, the material loses *instantaneously* its load bearing capability. By contrast, the criterion discussed in the present work considers the equivalent stress together with a *gradual loss* of load-bearing capability, all in the dynamic regime, specifically for adiabatic shear failure. Last but not least is the fact that the plastic strain energy density is based so far on physical evidence only, showing the role of the stored energy of cold work in adiabatic shear failure [7]. The reader is referred to the comprehensive work of Wierzbicki et al. [22] in which the C–L criterion was compared to other six fracture models. The C–L criterion was implemented in various numerical works specifically focused on fracture even though there was also ductility. For example, Álvarez et al. [23] used the C–L criterion to model chip formation during machining, and Børvik et al. [24] used it to model fragmentation and other fracture modes during ballistic penetration.

The second model, which also invokes energy concepts for the *onset* of flow localization in thermal viscoplastic materials, was postulated by Shawki [25], and [26]. This criterion is based on a *kinetic* energy density for the onset of localization (as opposed to *total* energy as in our work). In two later works [27,28] this criterion was used to qualitatively characterize the onset and propagation of shear bands. Unfortunately, no quantitative comparison is available for this criterion with experimental observations.

It is once again worth mentioning that the strain density energy failure criterion used in the earlier numerical works (Dolinski et al. [1] and Noam et al. [15]) describes *both* the critical condition for failure initiation and the *path to total fracture*. In another words, failure is not instantaneous. Rather it is characterized by a gradual decrease in the stress–strain relationship, resulting from damage evolution.

In this paper:

i. We present the algebraic formulation of the energy failure criterion. We compare it with the "classical" critical strain failure criterion, and show that the local stress–strain curve of the former decays in an approximately exponential manner, while that of the latter can be simply proved to decay linearly.
ii. For a particular case of the energy failure criterion ($b = 1$ and elastic-ideally plastic material), we show that the local decay is exactly exponential. Later on we discuss more general cases and show that the exponential decay criterion can still be applied partially.
iii. We show that this exponentially decaying local stress–strain relationship is supported by limited previous experimental as well as numerical results.
iv. Finally we show how to evaluate the required parameters from the local and macroscopic curves.

2. Formulation of failure criteria

2.1. Plastic strain energy density criterion

In both Dolinski et al. [1] and Noam et al. [15], the stress was assumed to evolve according to the amount of accumulated damage, D, as shown in Eq. (1)

$$\sigma_{eq} = \sigma_{eq}^{*} \cdot \left(1 - D^{b}\right) \tag{1}$$

where σ_{eq} is the current flow stress at a given equivalent strain (ε_{eq}), and σ_{eq}^{*} is the flow stress of the undamaged material for the current ε_{eq}. b is a constant.

The damage (D) evolution is given by Eqs. (2) and (3):

$$D = \begin{cases} 0 & W \le W_{cr} \\ \dfrac{W - W_{cr}}{W_f - W_{cr}} & W > W_{cr} \end{cases} \tag{2}$$

W is the plastic strain energy density for a strain level α:

$$W = \int_0^{\alpha} S_{ij} d\varepsilon_{ij}^{P} = \int_0^{\alpha} \sigma_{eq} d\varepsilon_{eq}^{P} \tag{3}$$

where S_{ij} is the deviatoric stress tensor and ε_{eq}^{P} is the plastic equivalent strain. W_{cr} is the critical value at which the material

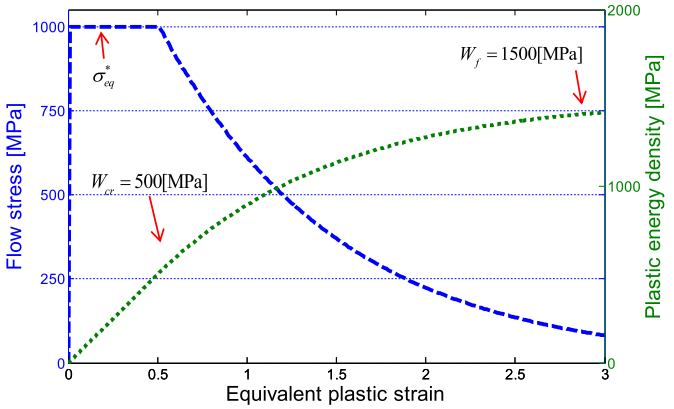

Fig. 1. Stress–strain curve of damage induced material (dashed line) and plastic strain energy density as a function of strain curve (dotted line). The curves corresponding material response for Eqs. (1)–(3) with the parameters: $\sigma^*_{eq} = 1000$[MPa], $W_{cr} = 500$[MPa], $W_f = 3 \cdot W_{cr} = 1500$[MPa] and $b = 1$.

starts to fail gradually until the fracture energy density W_f is reached, at which the material fully loses its load bearing capability.

The material response, as $\sigma_{eq} - \varepsilon^P_{eq}$ and $W - \varepsilon^P_{eq}$ curves, according to Eqs. (1)–(3), appears in Fig. 1. In this figure the material is elastic-ideally plastic, with a value of $\sigma^*_{eq} = 1000$[MPa], and it *starts to fail* at $W_{cr} = 500$[MPa], corresponding to a plastic strain $\varepsilon^p_{eq} = 0.5$. W_f is set arbitrarily as 3 times W_{cr}, i.e. $W_f = 1500$[MPa], and the parameter $b = 1$ as in Dolinski et al. [1].

This figure shows that the stress decays exponentially to zero, which is different from the strain criterion that decreases linearly (see Fig. 2 later on). A difference in behavior between these 2 criteria is contrary to what one would expect from an elastic-ideally plastic material especially when the exponent $b = 1$.

It is also seen that at $\varepsilon^p_{eq} \approx 3$, the flow stress is of the order of $0.1\sigma^*_{eq}$, which represents the typically observed very high strains and presumably low stresses in a shear band. It can also be noted from the figure that the plastic strain energy density rise rate (i.e. the power) diminishes, causing the plastic strain density energy itself to converge to the fracture energy parameter, $W_f = 1500$[MPa].

2.2. Critical strain criterion

The numerical implementation of a critical strain criterion is very common, due to the easy characterization from constitutive models and experiments, as exemplified in the seminal work of Molinari and Clifton [5]. A damage model based on this assumption is usually defined by two parameters, ε_{cr} which is the critical strain at which the material starts to fail, and a fracture strain ε_f for which the material has lost all or most of its load bearing capability. A numerical implementation of this damage model can be found in the work of Macdougall and Harding [29].

For comparison, the classical critical strain-based damage criterion is given by:

$$D = \begin{Bmatrix} 0 & \varepsilon_{eq} \le \varepsilon_{cr} \\ \dfrac{\varepsilon_{eq} - \varepsilon_{cr}}{\varepsilon_f - \varepsilon_{cr}} & \varepsilon_{eq} > \varepsilon_{cr} \end{Bmatrix} \tag{4}$$

$$\sigma_{eq} = \begin{Bmatrix} \sigma^*_{eq} & \varepsilon^P_{eq} \le \varepsilon_{cr} \\ \sigma^*_{eq} \cdot \left(1 - \dfrac{\varepsilon^P_{eq} - \varepsilon_{cr}}{\varepsilon_f - \varepsilon_{cr}}\right) & \varepsilon^P_{eq} > \varepsilon_{cr} \end{Bmatrix} \tag{5}$$

where ε_{cr} is the critical failure strain (onset of failure), and ε_f is the strain at total failure (fracture). D is zero up to ε_{cr}, and afterwards, as seen in Eq. (4), grows linearly to 1 for $\varepsilon_{eq} = \varepsilon_f$. A comparison of stress–strain curves for two damage criteria (strain and strain energy density) is shown in Fig. 2.

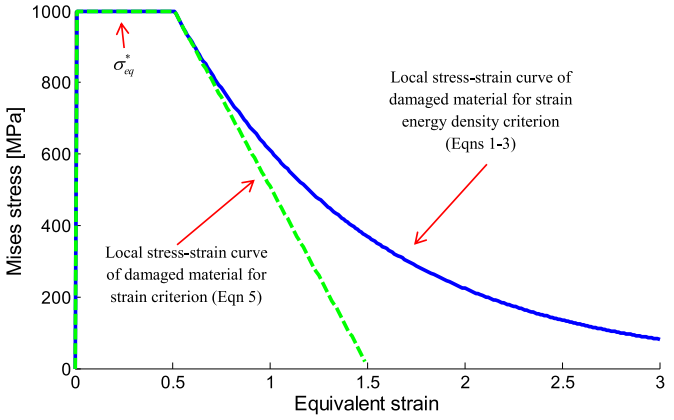

Fig. 2. Stress–strain curve of for two different damage criteria. The continuous curve is obtained from Eqs. (1)–(3) – strain energy density criterion, as in Fig. 1. The dashed curve is obtained from Eq. (5), with $\varepsilon_{cr} = 0.5$, and $\varepsilon_f = 3 \cdot \varepsilon_{cr} = 1.5$.

3. Analytical presentation of the stress strain relationship

In the previous section, the energy-based failure model was evaluated by iteratively processing Eqs. (1)–(3) in increments of strain. We now manipulate those equations, to obtain an analytical relationship between stress and strain, based on the energy criterion analogous to Eq. (5) obtained for the strain criterion.

We make 2 assumptions:

a. The material is assumed to be elastic-ideally plastic as before, with a constant σ^*_{eq} that independent of strain, strain-rate and temperature.
b. The parameter b is taken as 1.

Differentiating the damage Eq. (2), we obtain:

$$\mathrm{d}D = A \cdot \mathrm{d}W \tag{6}$$

where:

$$A = \frac{1}{W_f - W_{cr}} \tag{7}$$

Differentiating Eq. (3) and inserting (1) into the result, with $b = 1$, gives:

$$\mathrm{d}W = \sigma^*_{eq}(1 - D)\mathrm{d}\varepsilon^P_{eq} \tag{8}$$

Substituting (8) into (6) gives:

$$\frac{\mathrm{d}D}{\mathrm{d}\varepsilon^P_{eq}} = A \cdot \sigma^*_{eq} \cdot (1 - D) \tag{9}$$

Since σ^*_{eq} is assumed constant, integration of (9) gives an exponential solution:

$$D = 1 - \exp\left(-A \cdot \sigma^*_{eq} \cdot \left(\varepsilon^P_{eq} - \varepsilon_{cr}\right)\right) \tag{10}$$

where ε_{cr} is the equivalent plastic strain corresponding to the critical energy W_{cr}.

Substituting (10) into (1) gives the desired exponential decrease in stress:

$$\sigma_{eq} = \begin{cases} \sigma^*_{eq} & \varepsilon^P_{eq} \le \varepsilon_{cr} \\ \sigma^*_{eq} \cdot \exp\left(-\dfrac{\sigma^*_{eq}\left(\varepsilon^P_{eq} - \varepsilon_{cr}\right)}{W_f - W_{cr}} \right) & \varepsilon^P_{eq} > \varepsilon_{cr} \end{cases} \tag{11}$$

The exponentially decreasing stress–strain curve fails theoretically at infinite strain. Thus the value of the work (density) to failure W_f is not immediately attainable. However, if the natural logarithm of the stress is plotted against the strain, it can be seen from Eq. (9) that its slope will be:

$$\frac{\partial \ln(\sigma_{eq})}{\partial \varepsilon^p_{eq}} = -\frac{\sigma^*_{eq}}{W_f - W_{cr}} + C \tag{12}$$

where C is a constant.

Since σ^*_{eq} and W_{cr} are known, the parameter W_f can be easily determined from the experimental value of this slope, keeping in mind that $b = 1$.

To summarize we have shown analytically that for a material undergoing damage according to Eqs. (1) and (2), the stress–strain relationship is exponentially decaying.

4. Experimental justification of the stress exponential decay – literature survey

The direct measurement of *local* stress and strain fields in a material is quite delicate, especially when large strains and high strain rates are involved. In order to measure the true stress in a shear band, and at least have a rough estimate of the local strain, a torsional split Hopkinson bar can be used. This technique has been successfully used in the identification of the various stages of dynamic localization [3]. However, it is only recently that, with the progress of technology, a *real time local* stress–strain relation could be approximated.

Fellows and Harding [30] performed such an experiment, in which the local strains were measured using a high speed camera and a gridded specimen. The authors noted that while this being the best option to date, this procedure is still incomplete because a shear band nucleates at a certain point on the circumference of the specimen, and it propagates from there. The high speed camera is focused on a single area of the specimen and may well fail to capture the onset of that band. The same goes for the final fracture of the specimen. The assumption in such dynamic torsion experiments is that the shear stress is homogeneous in the gauge section, due to the axially-symmetric specimen geometry and boundary conditions. Fellows and Harding [30] worked on RHA (Rolled Homogeneous Armor), and measured an average strain rate of about $\dot{\varepsilon} \approx 1000[1/s]$ prior to localization. Only three out of the six reported experiments could be used to obtain a local stress–strain curve. Based on that data, a Mises stress versus equivalent strain curve of the localized material is presented in Fig. 3. This curve is a combination of the macroscopic shear stress over time and local shear strain over time curves for specimen B2 of Fellows and Harding [30]. One can observe the exponential decay of the material flow stress after exceeding the critical strain $\varepsilon^c_{eq} \approx 0.4$. The stress does not drop to zero, but if a natural logarithmic plot is performed as suggested earlier, the fracture strain energy density is estimated as: $W_f \approx 4 - 5\ W_{cr}$. This value is close to the (arbitrarily chosen) ratio of 3 used in previous work [1]. Unfortunately, this is the only available

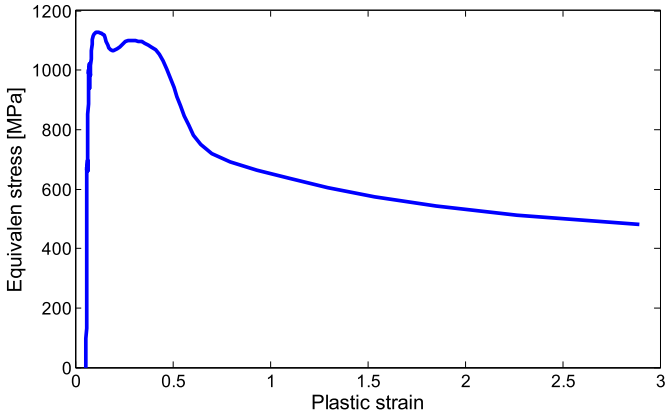

Fig. 3. Local stress–strain curves made from combination of stress and local strain curves over time of specimen B2 in the work of Fellows and Harding [30].

dynamic experiment which attempts to measure local material conditions in the shear band throughout the whole experiment. Therefore, this is just a validation for the exponential decay, rather than detailed verification of the entire model that should be based on more experimental evidence.

Another justification, albeit numerical, can be found in the works of Li et al. [31] and Zhou et al. [12], who modeled the material in the shear band as a Newtonian fluid. In this case, the flow stress decays exponentially with temperature. Keeping in mind that temperature and strain energy density are proportional, a damage evolution law is implemented, which is very similar to the one presented here. The reader is also referred to the works of Longère et al. [32] and of Longère and Dragon [33], who clearly obtain an exponential decay in their analytical and numerical works. Those authors also distinguish between the onset of failure (instability point), and abrupt drop in strength (localization point). This notion was earlier shown in the finite element solution of Wright and Batra [34], who report a gradual behavior of shear collapse until rapid stress drop. These observations are in line with our current work, as will be shown in the next section.

At this stage, it is important to further discuss and determine the two parameters that enter the damage model, namely the work to fracture, W_f, and the exponent b, as presented next.

5. Determination of the damage parameters

5.1. Determination on the damage exponent b

In our analytic development of the exponential decay criterion, we assumed b to be 1. Here we discuss the effects for other values of b.

Firstly we note that the value of b determines in fact the first stages of the failure, which are followed by fully formed adiabatic shear bands. As such, it can be viewed as a measure of the damage resistance, i.e. “toughness”, of the material. Fig. 4 illustrates this point by comparing local stress strain curves, generated using Eqs. (1)–(3), for 3 different values of b ($b = 1, 3$ and 10). The figure shows that: the factor b:

a. Influences the rapidity at which the material looses its load bearing capability.
b. Dictates the strain beyond which this catastrophic failure starts.
c. Determines the curvature of the graph once failure starts.

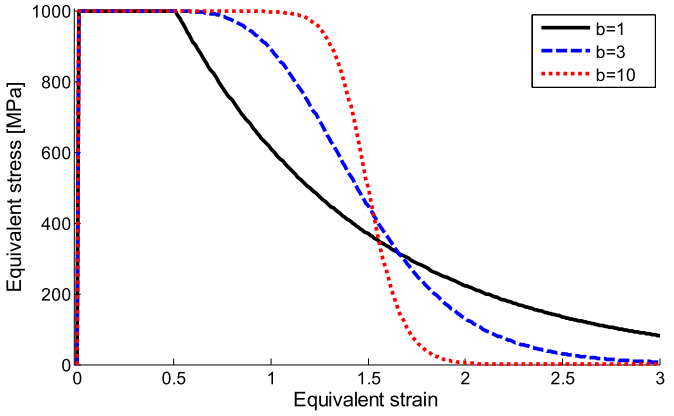

Fig. 4. Stress–strain curve of damaging materials with different values of the damage exponent b. The curves are generated using Eqs. (1)–(3) with: $\sigma^*_{eq} = 1000$[MPa], $W_{cr} = 500$[MPa], $W_f = 3 \cdot W_{cr} = 1500$[MPa], and $b = 1$, 3 and 10, respectively. Note that the continuous line is similar to the stress strain curve in Fig. 1 for $b = 1$.

Note that in all cases, the last stage of the failure shows an exponential decay. In all the three cases, the damage starts to evolve at the same strain energy density of $W_{cr} = 500$[MPa] (corresponding to $\varepsilon^p_{eq} = 0.5$). The fracture, i.e. total loss of load bearing capability, occurs in all the cases for $W_f = 3 \cdot W_{cr} = 1500$[MPa].

Noting these general characteristics, the value of b can be obtained from the macroscopic stress–strain curve as follows:

a. Two macroscopic stress–strain curves are built on one graph (Fig. 5): The experimental macroscopic average and that predicted from a calibrated reference constitutive model. In our case, we will select the widely used Johnson–Cook (J–C) model [35], applied to the experimental data reported by Marchand and Duffy [3].
b. At some point, the curves of Fig. 5 are seen to diverge. This is due to damaging of the material being reflected in the experimental curve, keeping in mind that the reference constitutive model does not include damage. A macroscopic damage parameter D_G can be defined based on the ratio between the measured (σ_{exp}) and reference stress (σ_{JC}):

$$D_G = 1 - \frac{\sigma_{exp}}{\sigma_{JC}} \tag{13}$$

The value of D_G is zero up to the onset of damage (divergence point in Fig. 5) and grows to one at fracture. A curve showing the evolution of D_G vs. strain energy density of the J–C reference constitutive model is shown in Fig. 6.

c. Against the experimental figure for D_G (Fig. 6) we define a theoretical "macroscopic damage" parameter D_G:

$$D_G = \begin{Bmatrix} 0 & W \le W_{cr} \\ \dfrac{W - W_{cr}}{W_f - W_{cr}} & W > W_{cr} \end{Bmatrix} \tag{14}$$

$$\sigma_{eq} = \sigma^*_{eq} \cdot \left(1 - D^b\right) \tag{15}$$

This equation is quite similar to Eq. (2). W is the same parameter of plastic strain energy density as defined in Eq. (3), W_{cr} – as before – is the critical strain energy density at which the material starts to fail, identified here as the divergence point. However, W_f, in this formulation, is the *macroscopic* energy to fracture rather than the *local* as described previously.

After defining the parameter D_G, it is possible to generate stress–strain curves for various values of b, keeping in mind that the parameter σ^*_{eq} in Eq. (15) is the J–C equivalent stress for undamaged material. This procedure is applied for 4 different values of b (1–4), as shown in Fig. 7, together with the experimental stress strain curve reported by Marchand and Duffy [3].

d. Fig. 7 shows that the best fit is obtained for $b = 3$, within the box framed region of interest. This region corresponds to the onset and propagation of damage, yet excluding the final phase of the failure process that corresponds to the abrupt drop in load bearing capability (stage III in Marchand and Duffy [3]).

Our choice of Marchand and Duffy's results [3] is not arbitrary. Their seminal experiment was successfully quantitatively modeled in our previous work Dolinski et al. [1]. The calibration procedure for the exponent b was not known back then. Therefore, both the

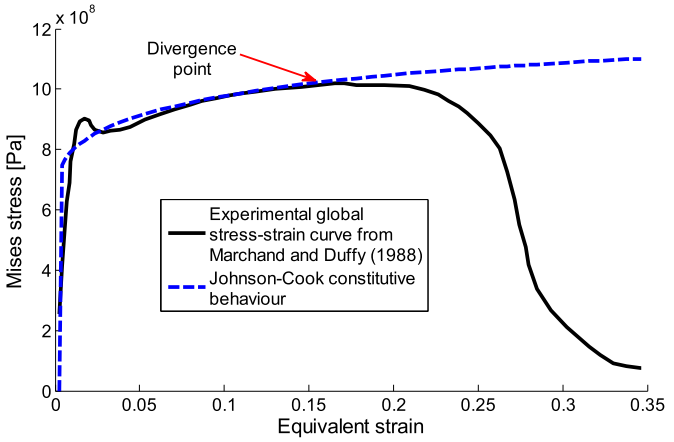

Fig. 5. Two stress–strain curves. The first one (continuous line) in taken from the work of Marchand and Duffy [3] and the second one (dashed) in Johnson Cook constitutive behavior of the same material.

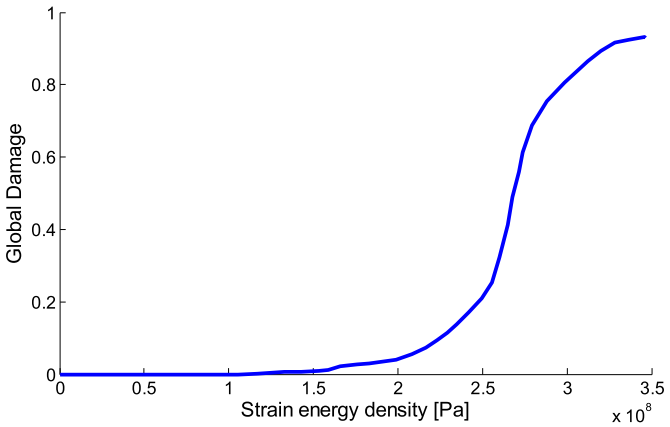

Fig. 6. The macroscopic damage D_G calculated using Eq. (13) as a function of strain energy density. The damage was set to zero until 100[MPa] to avoid small fluctuations arising from the experimental data.

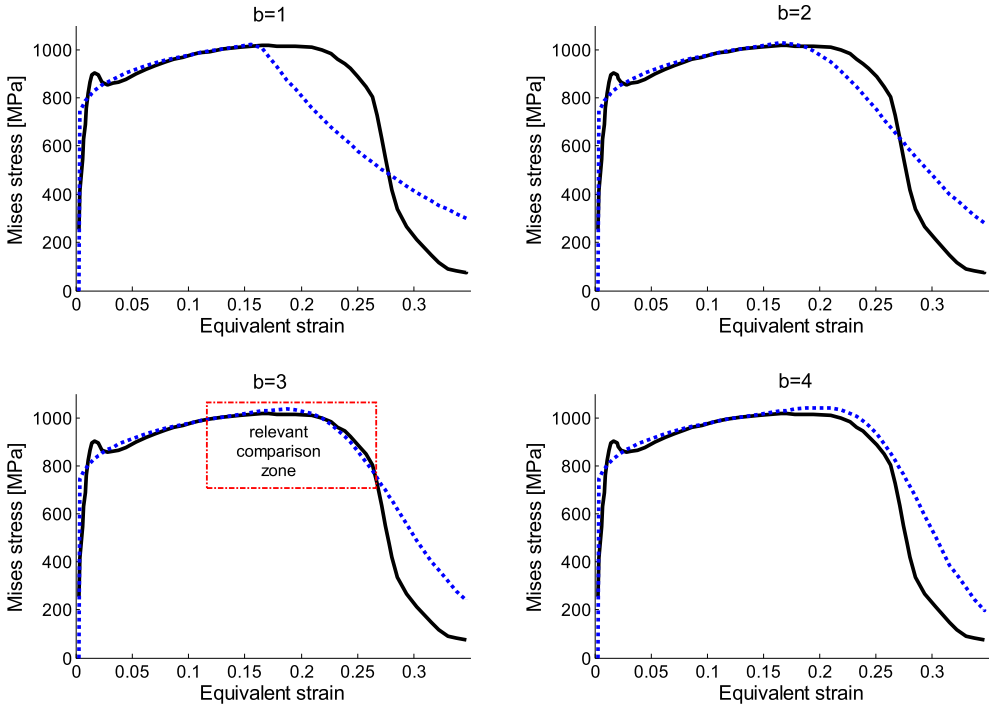

Fig. 7. Curves of stress strain curves for 4 different values of b (calculated using Eqs. (14) and (15), dashed line), compared to experimental curves [3].

parameters b and W_f were iteratively adjusted until the simulation recreated the global stress–strain curve. The adjusted parameter b which gave the best fit was 3, which is identical to the fitted value in the current procedure. W_f was adjusted to a value of 750[MPa].

5.2. Determination on the total strain energy density to fracture (W_f) for $b \neq 1$

Returning to the local curves of Fig. 4, we note that the decay at the last stages of failure seems to be exponential. Thus, the analytical part 3 in this article, in which $b = 1$ was postulated, might still be used, and may lead to a value of W_f.

We note that in the final stages of deformation, where the stress has already dropped significantly, the damage (D) is close to 1, Thus Eq. (8), for $b \neq 1$ becomes:

$$dW = \sigma^*_{eq}\left(1 - D^b\right)d\varepsilon^P_{eq} \rightarrow dW = \sigma^*_{eq} \cdot b \cdot (1 - D) d\varepsilon^P_{eq} \tag{16}$$

where only the first member of a Taylor series expansion is considered.

Repeating the analysis of section 3, we again obtain exponential decay, with Eq. (12) becoming this time:

$$\frac{\partial \ln(\sigma_{eq})}{\partial \varepsilon^p_{eq}} = -\frac{b \cdot \sigma^*_{eq}}{W_f - W_{cr}} + C \tag{17}$$

Eq. (17) is similar to Eq. (12), except that the new slope is now multiplied by the sought parameter b, keeping in mind this parameter must first be identified to determine W_f.

6. Discussion and conclusions

Our criterion for adiabatic shear localization, which was proposed and validated numerically in earlier works, is now analyzed rigorously. The criterion is formulated in terms of plastic strain energy density, as given by Eqs. (1)–(3). Those equations contain 2 parameters, b and W_f whose determination is addressed in the paper, in addition to the third parameter, W_{cr} that is directly determined from experimental data.

As a preliminary remark, damage (D), in this work, is to be considered as a general process through which the mechanical properties of the material are altered, more precisely lowered in the current case. We consider that prior to the shear band onset, the material is (virtually) undamaged. The evolving damage in the shear band accelerates its growth on the one hand, but also increases because of the shear band. From a physical point of view, one "damage" mechanism that was identified in earlier work relates to dynamic recrystallization [36] whereby soft nanograins are formed at the onset of the shear band. Damage can also be the result of thermal softening, the prime suspect in the literature about adiabatic shear. A thorough estimation of the relative contribution of microstructural evolutions e.g. DRX) and thermal softening can be found in the work of Osovski et al. [10]. This same work addresses the issue of the potential presence of "hot spots" in the sheared zone. Another form of damage might be microcracking, although the latter has not been reported to be present at the onset of the adiabatic shear band.

From a more general perspective, the damage, whatever its physical origin, has been shown to have a variable effect as a result of its spatial distribution (homogeneity), as shown in Ref. [37]. The damage parameter D lumps all those effects into a generic term.

While previous criteria (mentioned in the introduction) have been suggested, they generally address the *onset* of localization (e.g. critical strain) without specific emphasis on the following stages of the failure process, beyond the assumption of a linear stress–strain evolution. By contrast, the currently proposed criterion describes *both* the onset and evolution of the localization process by considering a critical value of the plastic strain energy density for the onset, and a specific exponential stress–strain relationship for the ensuing process. It is important to note that the notion of a critical strain energy density is based on earlier experimental work [7,9], and that the exponentially decaying stress strain relationship is now established based on physical observations as well.

An analytical solution is provided in Eq. (11) for the case where $b = 1$ for an elastic ideally-plastic material, which is rate and temperature-insensitive as well. This solution reveals the exponential character of the stress–strain relationship for the damaging material. Consequently, W_f can be directly determined from a *local* stress–strain relationship in the shear band. Unfortunately, such direct determinations are both very scarce and quite delicate to obtain experimentally. It is also shown that a critical strain criterion, as formulated in Eq. (11) can also be used with exponential stress–strain decay, for the case where $b = 1$ for this "ideal" material.

However, the above assumptions for the material properties are quite restrictive with respect to real materials. Therefore, the more general case of a rate and temperature-dependent material is examined next, together with the possibility that $b \neq 1$. In this case, the above procedure leading to Eq. (11) gets quite cumbersome and is therefore not pursued here. The conclusion is that Eqs. (1)–(3) must still be used, albeit with a numerical solution procedure.

The general nature of the parameter b is investigated by quantifying the evolution of the damage from both an experimental macroscopic stress–strain curve, and that fitted using any constitutive model (e.g. J–C) for the undamaged material, as illustrated in Fig. 7.

The value of the parameter b, as determined using this procedure, provides information on the damage tolerance of the material, namely the point at which the load bearing capacity collapses rapidly past a plateau period. Note that the final stage of failure corresponds again to the exponential decay which is at the core of this work. Once b is determined as described, W_f is the only adjustable parameter that could directly be determined from a *local* stress–strain curve, would it be available.

It is interesting to remark that we report here a value of $b = 3$ for Marchand and Duffy's experiments [3], a value that was empirically adjusted in our numerical calculations [1], providing a very good agreement between calculations and experiments.

The conclusion of this work is that a simple, physically based criterion for adiabatic (localized) shear failure has been proposed and thoroughly discussed in this work, whose main advantage is the small number of adjustable parameters to describe the overall sequence of damage initiation and growth in an impacted structure.

It is also important do perform additional experimental work centered around the determination of the local stress and strain fields in a shear band, in order to provide additional support to the suggested exponential stress–strain relationship in the damaging material.

References

[1] Dolinski M, Rittel D, Dorogoy A. Modeling adiabatic shear failure from energy considerations. J Mech Phys Solids 2010;58:1759–75.
[2] Bai Y, Dodd B. Shear localization: occurrence, theories, and applications. Oxford, UK: Pergamon Press; 1992.
[3] Marchand A, Duffy J. An experimental study of the formation process of adiabatic shear bands in a structural steel. J Mech Phys Solids 1988;36:251–83.
[4] Zener C, Hollomon JH. Effect of strain rate upon plastic flow of steel. J Appl Phys 1944;15:22–32.
[5] Molinari A, Clifton RJ. Analytical characterization of the shear localization in thermoviscoplastic materials. J Appl Mech 1987;54:806–12.
[6] Dormeval R, Ansart J. Adiabatic shear - influence of a predeformation. J Phys 1985;46:299–306.
[7] Rittel D, Wang ZG, Merzer M. Adiabatic shear failure and dynamic stored energy of cold work. Phys Rev Lett 2006;96:075502.
[8] Mazeau C, Beylat L, Longère P, Louvigné P. On the quantitative evaluation of adiabatic shear banding sensitivity of various titanium alloys. Le J Phys IV 1997;7. C3-429-C423-434.
[9] Rittel D, Wang Z. Thermo-mechanical aspects of adiabatic shear failure of AM50 and Ti6Al4V alloys. Mech Mater 2008;40:629–35.
[10] Osovski S, Rittel D, Venkert A. The respective influence of microstructural and thermal softening on adiabatic shear localization. Mech Mater 2013;56:11–22.
[11] Osovski S, Nahmany Y, Rittel D, Landau P, Venkert A. On the dynamic character of localized failure. Scr Mater 2012;67:693–5.
[12] Zhou M, Rosakis A, Ravichandran G. On the growth of shear bands and failure-mode transition in prenotched plates: a comparison of singly and doubly notched specimens. Int J Plast 1998;14:435–51.
[13] Medyanik S, Liu W, Li S. On criteria for dynamic adiabatic shear band propagation. J Mech Phys Solids 2007;55:1439–61.
[14] Xu Y, Chen J. Atomistic potentials based energy flux integral criterion for dynamic adiabatic shear banding. J Mech Phys Solids 2015;75:45–57.
[15] Noam T, Dolinski M, Rittel D. Scaling dynamic failure: a numerical study. Int J Impact Eng 2014;69:69–79.
[16] Aranda-Ruiz J, Loya JA. Numerical analysis of the brittle-ductile transition in the failure-mode in polymeric materials. In: Applied mechanics and materials. Trans Tech Publ; 2014. p. 310–5.
[17] Ravi-Chandar K, Lu J, Yang B, Zhu Z. Failure mode transitions in polymers under high strain rate loading. Int J Fract 2000;101:33–72.
[18] Sih GC. Strain-energy-density factor applied to mixed mode crack problems. Int J Fract 1974;10:305–21.
[19] Farren WS, Taylor GI. The heat developed during plastic extension of metals. Proc R Soc 1925;A107:422–51.
[20] Taylor GI, Quinney H. The latent energy remaining in a metal after cold working. Proc R Soc Lond 1934;143:307–26.
[21] Cockcroft M, Latham D. Ductility and the workability of metals. J Inst Met 1968;96:33–9.
[22] Wierzbicki T, Bao Y, Lee Y-W, Bai Y. Calibration and evaluation of seven fracture models. Int J Mech Sci 2005;47:719–43.
[23] Álvarez R, Domingo R, Sebastián MÁ. Investigation of Ti6Al4V orthogonal cutting numerical simulations using different material models. In: NUMIFORM 2010: proceedings of the 10th international conference on numerical methods in industrial forming processes dedicated to Professor OC Zienkiewicz (1921–2009). AIP Publishing; 2010. p. 787–94.
[24] Børvik T, Hopperstad OS, Pedersen KO. Quasi-brittle fracture during structural impact of AA7075-T651 aluminium plates. Int J Impact Eng 2010;37:537–51.
[25] Shawki T. An energy criterion for the onset of shear localization in thermal viscoplastic materials, part i: necessary and sufficient initiation conditions. J Appl Mech 1994;61:530–7.
[26] Shawki T. An energy criterion for the onset of shear localization in thermal viscoplastic materials, part ii: applications and implications. J Appl Mech 1994;61:538–47.
[27] Cherukuri H, Shawki T. An energy-based localization theory: I. Basic framework. Int J Plast 1995;11:15–40.
[28] Cherukuri H, Shawki T. An energy-based localization theory: II. Effects of the diffusion, inertia, and dissipation numbers. Int J Plast 1995;11:41–64.
[29] Macdougall D, Harding J. A constitutive relation and failure criterion for Ti6Al4V alloy at impact rates of strain. J Mech Phys Solids 1999;47:1157–85.
[30] Fellows N, Harding J. Localization of plastic deformation during high strain rate torsion testing of rolled homogeneous armour. J Strain Anal Eng Des 2001;36:197–210.
[31] Li S, Liu W-K, Qian D, Guduru PR, Rosakis AJ. Dynamic shear band propagation and micro-structure of adiabatic shear band. Comput Methods Appl Mech Eng 2001;191:73–92.
[32] Longère P, Dragon A, Trumel H, Deprince X. Adiabatic shear banding-induced degradation in a thermo-elastic/viscoplastic material under dynamic loading. Int J Impact Eng 2005;32:285–320.
[33] Longère P, Dragon A. Adiabatic heat evaluation for dynamic plastic localization. J Theor Appl Mech 2007;45:203–23.
[34] Wright TW, Batra RC. The initiation and growth of adiabatic shear bands. Int J Plast 1985;1:205–12.
[35] Johnson GR, Cook WH. A constitutive model and data for metals subjected to large strains, high strain rates and high temperatures. In: Proc. 7th int. symp. on ballistics, The Hague, The Netherlands (April 1983); 1983. p. 541–7.
[36] Rittel D, Landau P, Venkert A. Dynamic recrystallization as a potential cause for adiabatic shear failure. Phys Rev Lett 2008;101.
[37] Osovski S, Rittel D. Microstructural heterogeneity and dynamic shear localization. Appl Phys Lett 2012;101:211901.